Cancer Letters 459 (2019) 86–99

Contents lists available at ScienceDirect

Cancer Letters

journal homepage: www.elsevier.com/locate/canlet

Original Articles

Interferon-inducible lncRNA IRF1-AS represses esophageal squamous cell carcinoma by promoting interferon response

Jianbing Huang, Jiagen Li, Yuan Li, Zhiliang Lu, Yun Che, Shuangshuang Mao, Yuanyuan Lei, Ruochuan Zang, Sufei Zheng, Chengming Liu, Xinfeng Wang, Ning Li, Nan Sun**, Jie He*,[1]

Department of Thoracic Surgery, National Cancer Center/National Clinical Research Center for Cancer/Cancer Hospital, Chinese Academy of Medical Sciences and Peking Union Medical College, Beijing, 100021, China

ARTICLE INFO

Keywords:
Long non-coding RNA
Interferon
IRF1-AS
IRF1
Esophageal squamous cell carcinoma

ABSTRACT

Interferons (IFNs) play crucial roles in the development and treatment of cancer. Long non-coding RNAs (lncRNAs) are emerging molecules involved in cancer progression. Here, we identified and characterized an IFN-inducible nuclear lncRNA IRF1-AS (Interferon Regulatory Factor 1 Antisense RNA) which was positively correlated with IRF1 expression. IFNs upregulate IRF1-AS via the JAK-STAT pathway. Knockdown and overexpression of IRF1-AS revealed that IRF1-AS inhibits oesophageal squamous cell carcinoma (ESCC) proliferation and promotes apoptosis in vitro and in vivo. Mechanistically, IRF1-AS activates IRF1 (Interferon Regulatory Factor 1) transcription through interacting with ILF3 (Interleukin Enhancer Binding Factor 3) and DHX9 (DExH-Box Helicase 9). In turn, IRF1 binds to the IRF1-AS promoter directly and activates IRF1-AS transcription. Global analysis of IRF1-AS–regulated genes indicated that IRF1-AS activates the IFN response in vitro and in vivo. IRF1 knockdown in IRF1-AS–overexpressing cells abolished the antiproliferative effect and activation of the IFN response. Furthermore, IRF1-AS was downregulated in ESCC tissues, and low expression correlated with poor prognosis. In conclusion, the interferon-inducible lncRNA IRF1-AS represses esophageal squamous cell carcinoma progression by promoting interferon response through a positive regulatory loop with IRF1.

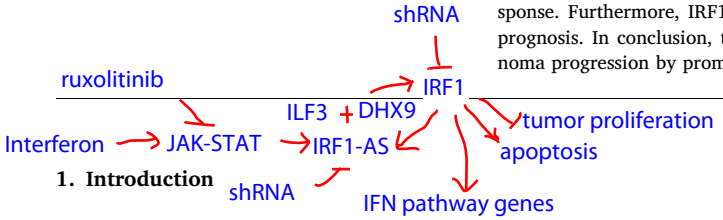

1. Introduction

Interferons (IFNs) are pleiotropic cytokines that have long been considered to be involved in the development and treatment of cancer. Interferons (IFNs) play crucial antitumor roles via their direct effects on cancer cells and activation of the immune response [1]. The binding of IFNs to their receptors activates the JAK-STAT pathway, resulting in the transcriptional activation of hundreds of IFN-stimulated genes (ISGs) [2]. Many ISGs directly affect the phenotypes of cancer cells, including cell proliferation, apoptosis, differentiation, survival and migration. In addition, IFNs have also emerged as central coordinators between tumors and the immune system. IFNs regulate the activation of almost all immune cell types, inducing a crucial immune response to malignant disease [1]. A pan-cancer analysis of the immune landscape indicates that the IFN-γ dominant immune subtype constitutes an important category of the tumor microenvironment, especially in esophageal carcinoma, highlighting the immunotherapeutic implications of IFNs [3]. IFNs regulate PD-L1 expression through the JAK/STAT/IRF1 axis and affect immunotherapy through checkpoint blockade [4,5]. The tumor-induced degradation of IFNAR1 promotes immune evasion, and stabilizing IFNAR1 could improve immunotherapy efficacy [6]. Although IFNs have pleiotropic effects on cancer, targeting the IFN pathway has been unsatisfactory due to difficulties in predicting patient sensitivity to any of the IFN types, thereby suggesting that some unknown mechanisms may underly the antitumor effects of IFNs.

Long non-coding RNAs (lncRNAs) constitute a large class of genome

Abbreviations: lncRNA, long non-coding RNA; IFN, interferon; IRF1, interferon regulatory factor 1; IRF1-AS, interferon regulatory factor 1 antisense RNA; DHX9, DExH-Box Helicase 9; ILF3, Interleukin Enhancer Binding Factor 3; ESCC, esophageal squamous cell carcinoma; shRNA, Short hairpin RNA; siRNA, Short interfering RNA; ChIP, chromatin immunoprecipitation; Co-IP, Co-Immunoprecipitation; RIP, RNA immunoprecipitation; RACE, rapid amplification of cDNA ends

* Corresponding author. Department of Thoracic Surgery, National Cancer Center/National Clinical Research Center for Cancer/Cancer Hospital, Chinese Academy of Medical Sciences and Peking Union Medical College, Beijing, 100021, China.

** Corresponding author. Department of Thoracic Surgery, National Cancer Center/National Clinical Research Center for Cancer/Cancer Hospital, Chinese Academy of Medical Sciences and Peking Union Medical College, Beijing, 100021, China.

E-mail addresses: sunnan@vip.126.com (N. Sun), prof.jiehe@gmail.com (J. He).

[1] Jie He will handle correspondence at all stages of refereeing and publication, also post-publication.

https://doi.org/10.1016/j.canlet.2019.05.038
Received 28 April 2019; Received in revised form 27 May 2019; Accepted 29 May 2019

transcripts that are greater than 200 bases with no apparent protein-coding role [7]. To date, mounting evidence supports that lncRNAs play important roles in cancer initiation and progression by affecting cancer cell proliferation, apoptosis, metastasis, metabolism and drug resistance [8,9]. LncRNAs regulate various levels of gene expression through *cis* or *trans* mechanisms by acting as decoys, guides, scaffolds or enhancers [9–11]. Although mechanistic models of lncRNAs in cancer have been widely proposed, to date, the functions and precise mechanisms of most lncRNAs remain unknown due to the large number of lncRNAs.

Some studies suggest that lncRNAs constitute an important subgroup of ISGs [12]. IFN-regulated lncRNAs regulate immune-related genes and may perform a function in the antiviral response [13,14]. However, the roles of IFN-regulated lncRNAs in cancer and their interactions with the IFN pathway remain unclear. Therefore, we comprehensively analyzed IFN-regulated lncRNAs and identified a novel nuclear lncRNA (IRF1-AS), which was functionally characterized as a tumor suppressor and positive regulator of the IFN response in ESCC.

2. Materials and methods

2.1. Patients and tissue samples

Fresh-frozen tissues, including 48 ESCC tissues and 38 adjacent normal tissues, were obtained at the Cancer Hospital of the Chinese Academy of Medical Sciences in 2012. A paraffin-embedded ESCC tissue microarray (TMA) (Catalogue No. ESC77) of 225 patients was purchased from Superbiotek, Inc. (China). The patients represented in the TMA underwent tumor resection in 2014 and were followed up until June 2017. All samples were collected with signed informed consent and were approved by the Ethics Committee of the Cancer Hospital of the Chinese Academy of Medical Sciences.

2.2. Cell culture

The ESCC cell lines were cultured in RPMI 1640 medium (HyClone), and the Het-1A esophageal epithelial cells were cultured in BEGM BulletKit medium (Lonza/Clonetics). The RPMI 1640 medium was supplemented with 10% FBS (Gibco), penicillin (100 U/mL) and streptomycin (100 mg/ml). All cell lines used in our study were regularly authenticated by short tandem repeat (STR) profiling.

IFN-β (Catalogue No. P01574, R&D) and IFN-γ (Catalogue No. CAA31639, R&D) were used at 1000 IU/ml. In the experiments involving ruxolitinib (Catalogue No. S1378, Selleckchem), the ESCC cells were treated with ruxolitinib (2 μM) for 1 h prior to the addition of IFN-β and then cultured for 12 h.

2.3. RNA extraction and quantitative real-time polymerase chain reaction (RT-qPCR)

The total RNA was extracted from the cultured cells by using a standard TRIzol protocol (Thermo Fisher Scientific). The cytoplasmic and nuclear RNAs were extracted and purified using a Protein and RNA Isolation System (Thermo Fisher Scientific) according to the manufacturer's instructions. Complementary DNA (cDNA) was synthesized using a RevertAid First-Strand cDNA Synthesis Kit (Thermo Fisher Scientific), and quantitative RT-PCR (RT-qPCR) was performed on an ABI 7900HT Real-Time PCR Thermocycler (Life Technologies). We used the $2-\Delta\Delta Ct$ method to quantify the relative RNA expression level, and GAPDH was used as an endogenous reference. At least two independent experiments were conducted with a minimum of three technical replicates per experiment. All primers and oligonucleotides used in this study are listed in Supplementary Table S1.

2.4. Western blotting and co-immunoprecipitation

The proteins were isolated from the cultured cells using RIPA buffer supplemented with a protease and phosphatase inhibitor cocktail and quantified with a BCA protein assay kit (Thermo Fisher Scientific). Identical amounts of proteins were separated by sodium dodecyl sulfate-polyacrylamide gel electrophoresis and transferred onto polyvinylidene fluoride (PVDF) membranes (Millipore). The membranes were blocked with 5% nonfat milk for 1 h at room temperature. After incubation with specific primary antibodies overnight at 4 °C, the blots were incubated with an HRP-conjugated secondary antibody and detected using AmershamTM Imager 600 (GE).

The co-immunoprecipitation assays were performed using a Pierce™ Classic Magnetic IP/Co-IP Kit (Catalogue No. 88804, Thermo Fisher Scientific) according to the manufacturer's instructions. All antibody information is listed in Supplementary Table S2.

2.5. Plasmid transfection and RNA interference

Two short hairpin RNAs (shRNAs) targeting the IRF1-AS non-overlapping region with IRF1 were cloned into a pLKO.1-puro vector, and full-length IRF1-AS cDNA was inserted into a pCDH-CMV-MCS-EF1-GFP + Puro (CD513B-1) vector (Generay, China). Then, the recombinant plasmids and packaging plasmids (pLP1, pLP2 and pLP/VSVG; Thermo Fisher Scientific) were co-transfected into HEK-293T cells to obtain infectious lentivirus particles according to the standard Lipofectamine 3000 instructions (Thermo Fisher Scientific). The lentivirus-containing supernatant was collected at 48 h and purified with Amicon Ultra-4 Centrifugal Filter Devices (Millipore). The purified lentivirus was supplemented with 5 μg/ml polybrene (Sigma-Aldrich) and used to infect the ESCC cells. We used corresponding empty vectors as controls. Stable cell lines were obtained after 14 days of selection with puromycin.

Small interfering RNAs (siRNAs) were designed to target IRF1 in the non-overlapping region with IRF1-AS. The siRNAs were synthesized by Sangon Biotech (China). The ESCC cells were seeded into 6-well plates and transfected with 50 pmol siRNA using RNAiMAX (Life Technologies) according to the manufacturer's instructions and harvested 48 h post-transfection.

2.6. Cell proliferation and colony formation assays

CCK8 assays (Dojindo, Japan) were performed according to the manufacturer's instructions. Briefly, the cells (1500 cells/well for KYSE30, 3000 cells/well for KYSE180) were seeded into 96-well plates, and the OD values were measured at 0, 24, 48, 72, 96 and 120 h. For the colony formation assay, 200 cells were seeded into 6-well plates and cultured for 10–14 days; the colonies were fixed and stained with 1% crystal violet.

2.7. Apoptosis induction assay

The ESCC cells were seeded into 6-well plates, cultured for 24 h and then treated with cisplatin (10 μM) for 24 h. The apoptotic cells were double-labeled with annexin V–allophycocyanin (APC) and propidium iodide (PI) using an apoptosis detection kit (KeyGEN BioTECH, China) according to the manufacturer's instructions.

2.8. Immunohistochemistry (IHC) and TUNEL assay

Briefly, the paraffin-embedded xenograft tumors were sectioned and stained with hematoxylin and eosin (H&E) and primary antibodies. TUNEL (Terminal deoxynucleotidyl transferase dUTP nick end labeling) assays were performed using a DeadEndTM Fluorometric TUNEL System according to the manufacturer's instructions.

2.9. In vivo animal experiments

To generate the xenograft model, 4-week-old athymic BALB/c nude

mice (Huafukang Bioscience, China) were subcutaneously injected with 2×10^6 KYSE30 cells into their right flank. The tumor length (a) and minor diameter (b) were measured once a week. The tumor volume was calculated using formula $V = ab^2/2$. After the tumors grew for 4–5 weeks, the mice were euthanized, and the tumors were harvested, weighed and analyzed. The animal studies were approved by the Animal Care and Use Committee of the Cancer Hospital of the Chinese Academy of Medical Sciences.

2.10. Analysis of 5′ and 3′ rapid amplification of cDNA ends (RACE)

Subsequently, 3′ RACE and 5′ RACE were performed using a SMARTer™ RACE cDNA Amplification Kit (Clontech, CA) and GeneRacer RLM-RACE Kit (Invitrogen), respectively, according to the manufacturers' instructions. The products of the 5′-RACE and 3′-RACE PCR were cloned into a pEASY-Blunt Zero vector with a pEASY-Blunt Zero Cloning Kit (TransGen, China) according to the manufacturer's instructions. At least three colonies were sequenced per gel product.

2.11. RNA in situ hybridization (ISH)

For the in situ detection of lncRNA IRF1-AS in ESCC cells and tissue microarray sections, an IRF1-AS probe targeting the non-overlapping region with IRF1 was designed and produced by Advanced Cell Diagnostics (Catalogue No. 549141, ACD). The hybridization and signal detection were performed using an RNAscope Detection Kit (Catalogue No. 322300, ACD) according to the manufacturer's protocol. Confocal laser scanning microscopy (Leica) was used to observe the expression of IRF1-AS. The specific IRF1-AS ISH signal was identified as brown, punctate dots, and the expression level was scored as follows: 0 = no staining or less than 1 dot per 10 cells, 0.5 = 10%–50% of cells displaying 1 dot, 1 = more than 50% of cells displaying 1 dot or 1 to 3 dots per cell, 2 = 4 to 9 dots per cell (few or no dot clusters), 3 = 10 to 14 dots per cell (less than 10% in dot clusters), and 4 = greater than 15 dots per cell (more than 10% in dot clusters). For each evaluable tissue spot, a final cumulative score was obtained as the sum of the individual products of the expression level (0–4) and percentage of cells (0–100) (i.e., [A% × 0] + [B% × 0.5] + [C% × 1] + [D% × 2] + [E% × 3] + [F% × 4]; total range = 0 to 400). The expression levels of IRF1-AS were defined as high (score > 50) or low (score ≤ 50), based on the distribution of the IRF1-AS expression level.

2.12. Chromatin immunoprecipitation (ChIP) assay

The ChIP assays were performed with a SimpleChIP® Enzymatic Chromatin IP Kit (CST) according to the manufacturer's instructions. The cells were treated with IFN-β or PBS for 6 h prior to ChIP assays involving interferon stimulation.

For the RNase ChIP assay, KYSE30 cells were permeabilized and treated with RNase before performing the standard ChIP assay. Briefly, the cells were obtained by centrifugation, permeabilized in 0.3% Triton X-100, and then treated with 20 mg/ml RNase A (Life Technologies), 1000 U/ml RNase H (NEB) or 1000 U/ml RNase inhibitor (NEB) for 30 min at 37 °C. Following the RNase treatment, an aliquot (80% vol) was processed for the ChIP assay, and the remaining aliquot (20% vol) was processed for RNA extraction.

2.13. RNA pull-down and mass spectrometry assay

The RNA pull-down assays were performed using a Pierce™ Magnetic RNA-Protein Pull-Down Kit (Thermo Fisher Scientific) according to the manufacturer's instructions. First, IRF1-AS was transcribed in vitro from the linearized vector pGEMT-easy-IRF1-AS using a HyScribe T7 High Yield RNA Synthesis Kit (NEB). Then, IRF1-AS and the negative RNA control [poly(A)25 RNA] were labeled with biotinylated cytidine bisphosphate, captured using streptavidin magnetic beads, and incubated with cell lysate. The eluted RNA-binding protein complexes from IRF1-AS and the negative RNA control were sent to CapitalBio Technology (China) for mass spectrometry detection.

2.14. RNA immunoprecipitation (RIP) assay

The RIP experiments were performed with a Magna RIP™ RNA-Binding Protein Immunoprecipitation Kit (Millipore) according to the manufacturer's instructions. Briefly, KYSE30 cells were lysed in complete RIP lysis buffer, and the cell extract was incubated with magnetic beads conjugated with specific antibodies or IgG overnight at 4 °C. The beads were washed and incubated with Proteinase K to remove the proteins. The purified RNAs were analyzed by RT-qPCR.

2.15. Dual luciferase reporter assay

The IRF1-AS promoter was cloned into the pGL4.10 vector, and cDNA was cloned into the pcDNA3.1(+) vector. The mutant vectors were obtained using a QuikChange Lightning Multi Site-Directed Mutagenesis Kit (Agilent Technologies). The luciferase activities were detected using a Dual-Luciferase Reporter Assay System (Promega) and normalized to Renilla. The sequence ranging from 2000 bp upstream to 100 bp downstream of the transcription start site was considered the promoter region.

2.16. RNA sequencing

The IFN-β-treated and control KYSE30, KYSE180 and KYSE450 cells and the IRF1-AS knockdown and control KYSE30 and KYSE180 cells were used to perform RNA sequencing (RNA-seq). RNA-seq was performed using Illumina HiSeq 4000 and was carried out by Novogene (China). Briefly, TopHat was used to map the reads to the reference genome (hg38), and HTSeq was used to count the number of reads mapped to each gene. The reference genome and gene annotation files were downloaded from Ensembl. The RNA-seq data obtained in this study were submitted to the NCBI Gene Expression Omnibus (GEO) under accession number GSE124514.

2.17. Statistical analysis

The statistical analyses were performed using SPSS version 19.0. All data are presented as the mean ± standard deviation. Student's t-test (two-tailed) was used to analyze the experiments involving only two groups, and one-way ANOVA was used to analyze the experiments involving three or more groups. The Mann-Whitney *U* test was performed for the comparisons of the xenograft tumor weights and volumes. The overall survival was estimated by using the Kaplan-Meier method and compared using the log-rank test. The Chi-square test was used to analyze the relationship between IRF1-AS expression and the clinicopathological characteristics. The differences were considered significant at $P < 0.05$, $^{***}P < 0.001$, $^{**}P < 0.01$, and $^{*}P < 0.05$ (ns, not significant).

3. Results

3.1. Identification of nuclear lncRNA-IRF1-AS as an IFN-inducible lncRNA via JAK-STAT pathway

To illustrate the potential role of IFN-regulated lncRNAs in ESCC, we performed an RNA-seq analysis of IFN-β-treated and control ESCC cells. We treated the ESCC cell lines KYSE30, KYSE180 and KYSE450 with 1000 U/ml recombinant IFN-β for 72 h prior to RNA-seq. Before performing RNA-seq, we first confirmed that the known ISGs, i.e., Mx1 and ISG15, were significantly upregulated after the IFN-β stimulation (Supplementary Fig. S1). The RNA-seq results indicated that some known protein-coding ISGs, including RSAD2 (Radical S-Adenosyl

ruxolitinib → Interferon → JAK-STAT → IRF1 + IRF1-AS

6 top RT-qPCR; most significant induction: RP11-89G4.1

ESCC cell lines: KYSE30, KYSE180, KYSE450

IFN-β 72 h + RNA-seq (Illumina HiSeq 4000)

positive correlation: IRF1 vs IRF1-AS

(Rapid Amplification of cDNA Ends)
*3'-RACE + oligo dT
*5'-RACE: Reverse transcriptase add a few C residues + oligo dG as primer

Strand-specific end-point PCR:
*high fidelity polymerase(Pfu)
*uracil-DNA glycosylase (UDG)

primer

IRF1-AS in nucleus

RNAscope (RNA FISH)

Interferon → IRF1-AS (nucleus)

(type I interferon)

I(type II interferon)

cytoplasm marker

IRF1-AS promoter

ChIP-seq

anti-STAT antibodies retrieved from the ENCODE project (Encyclopedia of DNA Elements)

Ruxolitinib: JAK inhibitor

ChIP-qPCR

anti-STAT1 antibody in KYSE30 cells

Bait: STAT1, STAT2, STAT3 antibody
PCR: IRF1-AS promoter region

(caption on next page)

Fig. 1. Identification of the IFN-regulated nuclear lncRNA IRF1-AS in ESCC. (A) Venn diagram of the upregulated and downregulated lncRNAs after the IFN-β induction in three ESCC cell lines. (B) Expression profiles of differentially regulated lncRNAs (over 2-fold change in expression) in three ESCC cell lines. (C) and (D) The Pearson correlation coefficient between IRF1-AS (RP11-89G4.1) and IRF1 in ESCC cell lines (C) and ESCC tissues (D) as detected by RT-qPCR. The data are shown as the mean ± SD. (E) Schematic representation of the IRF1-AS and IRF1 locus in the human genome. IRF1 is shown in black; public assembly of an EST of IRF1-AS is shown in light grey; the portions extended through RACE are shown in red, with a poly(A) tail in the 3′ end. The arrowheads define the orientation of the sequences. The number 1 and 2 indicate primers of IRF1-AS and IRF1. The grey numbers indicate start site of IRF1-AS exon 1 and end site of exon 3 in human genome. (F) Strand-specific end-point PCR of IRF1-AS in ESCC cell lines with antisense (AS) and sense (S) reverse-transcription (RT) primers relative to IRF1. RT reactions without primers were used as a negative control (Ctl). (G) Subcellular location of IRF1-AS. U99 and GAPDH are nuclear and cytoplasmic markers, respectively. (H) Confocal RNAscope images showing the nuclear localization of IRF1-AS in KYSE30 and KYSE180. The RNAscope kit's positive and negative controls were used. (I) Time course curvilinearity of the IRF1-AS expression level after the IFN-β and IFN-γ stimulation. (J) Expression level of IRF1-AS after the treatment with the JAK inhibitor ruxolitinib (Ruxo). ESCC cells were treated with ruxolitinib (2 μM) for 1 h prior to the addition of IFN-β (1000 IU/ml) and then cultured for 12 h. The plus and minus signs at the bottom represent the added or omitted ingredient, respectively. Ruxo, ruxolitinib. (K) ChIP-seq results using anti-STAT antibodies retrieved from the ENCODE project. (L) ChIP-qPCR assay using an anti-STAT1 antibody in KYSE30 cells. KYSE30 cells were treated with IFN-β or PBS for 6 h prior to the ChIP assay. Primers specific for ChIP-seq signal peak were used for ChIP-qPCR. The data are shown as the mean ± SD. P-values were obtained using Student's t-test (2 tailed). ***P < 0.001, **P < 0.01, *P < 0.05. (For interpretation of the references to colour in this figure legend, the reader is referred to the Web version of this article.)

Methionine Domain Containing 2), IFIT1(Interferon Induced Protein With Tetratricopeptide Repeats 1), IFIT3 (Interferon Induced Protein With Tetratricopeptide Repeats 3), Mx2 (MX Dynamin Like GTPase 2) and ISG15 (ISG15 Ubiquitin-Like Modifier), were significantly upregulated in the IFN-β-treated cells (Supplementary Fig. S2A). The gene set enrichment analysis (GSEA) of the protein-coding genes demonstrated an enrichment of the interferon response (Supplementary Fig. S2B), cell cycle and apoptosis (Supplementary Fig. S2C), which were consistent with the IFN effects [1]. Therefore, the ESCC cells exhibited the appropriate biological response to the IFN-β stimulation in our study.

The analysis of the expression changes in the lncRNAs indicated that 499 lncRNAs were upregulated and 495 lncRNAs were downregulated among the three IFN-β-treated cell lines (Fig. 1A). To the best of our knowledge, the biological function of these IFN-regulated lncRNAs remains largely unknown (Fig. 1B). Among the upregulated lncRNAs (Fig. 1B), GAS5 has been previously reported to be regulated by the IFN pathway and play an antitumor role in ESCC [15]. Then, we confirmed the IFN-β-mediated upregulation of the 6 top-ranked lncRNAs using RT-qPCR (Supplementary Fig. S3).

Among the identified lncRNAs, an RNA annotated as RP11-89G4.1 (ENSG00000277192) showed the most significant induction after the IFN stimulation (Supplementary Fig. S3). RP11-89G4.1 was transcribed from the antisense strand in the opposite direction relative to IRF1 (interferon regulatory factor 1). IRF1 is an extensively characterized ISG and a central regulator of the IFN response [16]. Subsequently, we initially investigated the possible relationship between RP11-89G4.1 and IRF1 by examining their correlation in a panel of human ESCC cell lines. The results revealed a positive correlation between the RP11-89G4.1 and IRF1 RNA levels (Fig. 1C). Then, we further confirmed their positive correlation in 48 fresh-frozen ECSS tissues (Fig. 1D). Moreover, RP11-89G4.1 and IRF1 were positively correlated in several other cancer types in addition to ESCC, including lung cancer, breast cancer and head and neck squamous cell carcinoma according to data retrieved from The Atlas of Non-coding RNA in Cancer (TANRIC) online database (Supplementary Fig. S4) [17]. Therefore, we focused on this lncRNA and named it IRF1-AS (Interferon Regulatory Factor 1 Antisense RNA).

To unravel the potential role of IRF1-AS in ESCC, we first performed RACE to obtain the full sequence of IRF1-AS, which was 2633 nucleotides with a poly(A) tail (Fig. 1E and Supplementary Fig. S5). IRF1-AS has 3 exons, and exon 3 has a region overlapping with IRF1 (Fig. 1E). Then, we confirmed that IRF1-AS was transcribed from the antisense strand in the ESCC cell lines using strand-oriented RT-PCR (Fig. 1F). Subsequently, we detected the subcellular localization of IRF1-AS with nuclear and cytoplasmic RNA fractions using RT-qPCR. We found that IRF1-AS was mainly enriched in the nucleus (Fig. 1G). Moreover, we confirmed the nuclear localization of IRF1-AS using RNA ISH (Fig. 1H). Although ORF Finder (National Center for Biotechnology Information) predicted that a protein of 149 amino acids was translated from IRF1-AS (Supplementary Fig. S6A), only one low homology protein was found using NCBI BLAST (Supplementary Fig. S6A), indicating that the predicted protein translated from IRF1-AS was of low credibility. IRF1-AS also showed negative codon substitution frequency scores (Supplementary Fig. S6B), indicating that it is a non-coding RNA [18]. Collectively, these results indicate that IRF1-AS is an independent nuclear non-coding transcript.

To determine whether IRF1-AS was a bona fide ISG, we found that both IFN-β (type I interferon) and IFN-γ (type II interferon) could induce IRF1-AS expression at 24, 48 and 72 h (Fig. 1I). IFNs upregulate ISGs mainly through the classical JAK-STAT pathway [1,19]. The binding of IFNs to their receptors leads to the phosphorylation of JAK proteins, resulting in the phosphorylation and nuclear translocation of STATs [1]. To determine whether IFNs induce IRF1-AS via the JAK-STAT pathway, we treated ESCC cells with the JAK inhibitor ruxolitinib. The results indicated that ruxolitinib abrogated the IFN-β-mediated upregulation of IRF1-AS (Fig. 1J). Then, we retrieved the ChIP-seq results using anti-STAT antibodies from the ENCODE project using IGV software (Integrative Genomics Viewer, v_2.4.11) and found that the transcriptional factors STAT1, STAT2 and STAT3 all had binding peaks around the IRF1-AS promoter region in several cell types (Fig. 1K). Furthermore, we performed a ChIP-qPCR assay using an anti-STAT1 antibody to confirm the ChIP-seq results in KYSE30. The results showed that STAT1 binds the IRF1-AS promoter and that IFN-β stimulation may promote this interaction (Fig. 1L). Taken together, these results demonstrate that IRF1-AS is a polyadenylated nuclear lncRNA induced by IFNs via the JAK-STAT pathway.

3.2. IRF1-AS inhibits ESCC proliferation and promotes apoptosis in vitro and in vivo

To investigate the function of IRF1-AS in ESCC, we stably knocked down IRF-AS using hairpin RNAs (shRNAs) targeting the non-overlapping region with IRF1 in KYSE30 and KYSE180 (Fig. 2A). Then, we performed CCK8 assays to compare the cell viabilities of the IRF1-AS knockdown and control cells and found that the viability of the knockdown cells was significantly promoted (Fig. 2B). The colony formation assays also demonstrated promoted colony formation in the knockdown cells (Fig. 2C). We further investigated whether IRF1-AS was involved in the regulation of cell apoptosis by performing flow cytometry. We found that the knockdown of IRF1-AS inhibited cisplatin-induced cell apoptosis (Fig. 2D). Moreover, our results showed that the knockdown of IRF1-AS had no significant effects on the migration and invasion ability of the ESCC cells in vitro (Supplementary Fig. S7).

To investigate the in vivo function of IRF1-AS, we constructed a xenograft model through percutaneous injections of IRF1-AS knockdown cells or control cells into nude mice. The results showed that the tumors grown from IRF1-AS knockdown cells exhibited increased

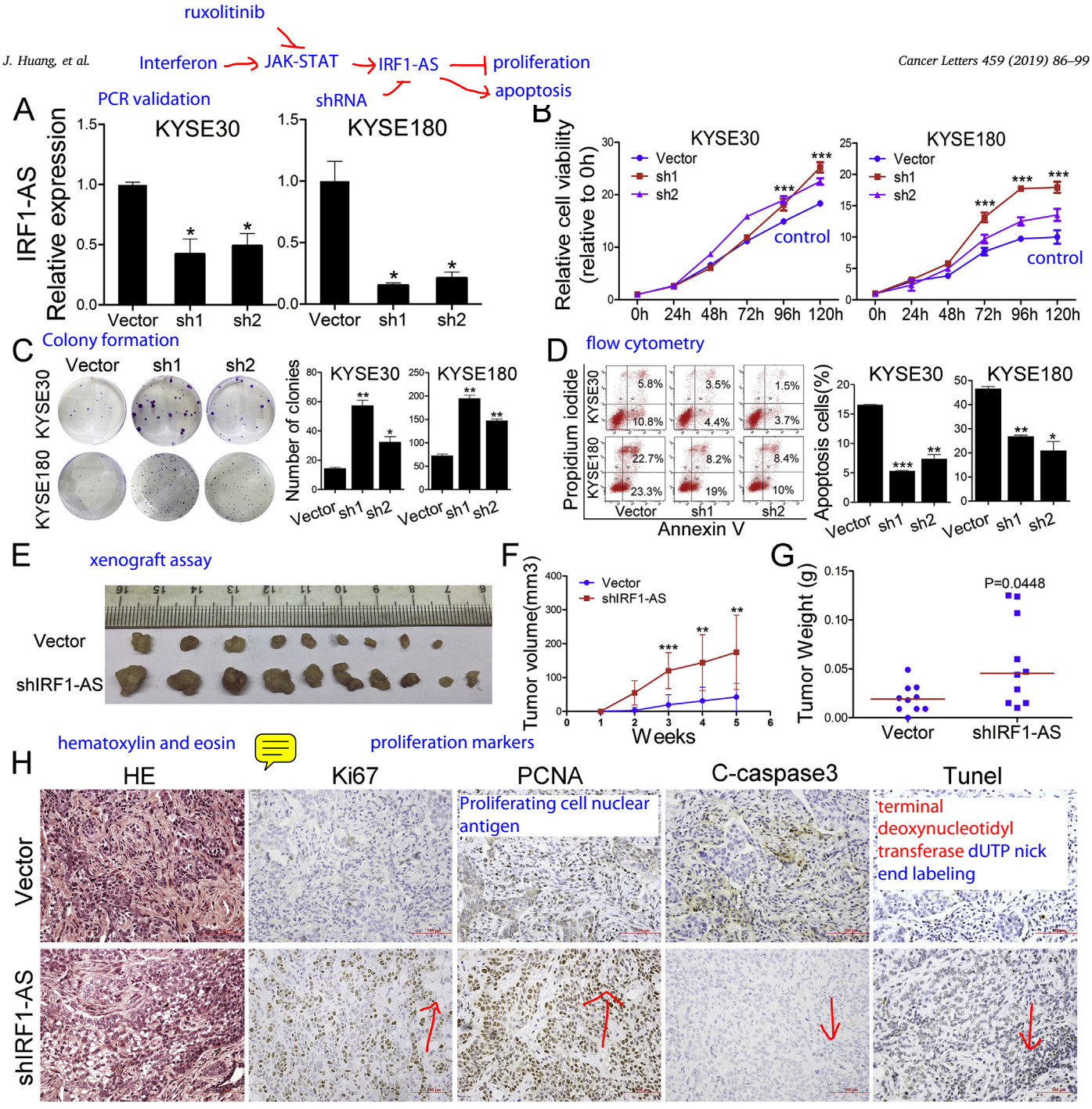

Fig. 2. Knockdown of IRF1-AS promotes ESCC proliferation and inhibits apoptosis in vitro and in vivo. (A) Validation of the IRF1-AS knockdown efficiency by RT-qPCR in KYSE30 and KYSE180 cells. (B) Proliferation assays of IRF1-AS-knockdown cells and vector control cells. P-values were obtained using one-way ANOVA. (C) Colony formation assays of IRF1-AS-knockdown cells. The right panel shows the quantification results. (D) FACS analysis of the effect of IRF1-AS knockdown on cell apoptosis. (E) Images, (F) volumes and (G) weights of xenografts established by the subcutaneous transplantation of IRF1-AS-knockdown and control KYSE30 cells. (H) Representative images of hematoxylin and eosin (H&E), immunohistochemistry (IHC) and terminal deoxynucleotidyl transferase dUTP nick end labeling (TUNEL) staining of paraffin-embedded sections obtained from xenografts. C-caspase 3, cleaved caspase 3. Original magnification, × 200. The data are shown as the mean ± SD. ***P < 0.001, **P < 0.01, *P < 0.05.

tumor volumes (Fig. 2E and F) and tumor weights (Fig. 2G). Moreover, the IHC staining showed that the IRF1-AS knockdown tumors presented an increased expression of the proliferation markers Ki67 and PCNA and decreased expression of the apoptosis marker cleaved caspase 3 (Fig. 2H). The TUNEL assays further confirmed the decreased number of apoptotic cells in the IRF1-AS knockdown tumors (Fig. 2H). Taken together, these results suggest that IRF1-AS plays a tumor suppressive role in vitro and in vivo.

To further confirm the tumor suppressive role of IRF1-AS, we stably overexpressed IRF1-AS in KYSE30 and KYSE180 cells (Fig. 3A). The CCK8 and colony formation assays showed that the overexpression of IRF1-AS impaired ESCC cell proliferation (Fig. 3B) and colony formation (Fig. 3C). The apoptosis analysis indicated that the overexpression of IRF1-AS promoted cisplatin-induced cell apoptosis in vitro (Fig. 3D). Further in vivo xenograft results showed that the IRF1-AS overexpression tumors exhibited decreased tumor volumes (Fig. 3E and F) and tumor weights (Fig. 3G). Furthermore, the IHC staining and TUNEL assays of the xenografts confirmed that the overexpression of IRF1-AS inhibited tumor growth and promoted tumor apoptosis (Fig. 3H). Altogether, these results demonstrate that IRF1-AS may inhibit tumor growth in vitro and in vivo by functioning as a tumor suppressive lncRNA.

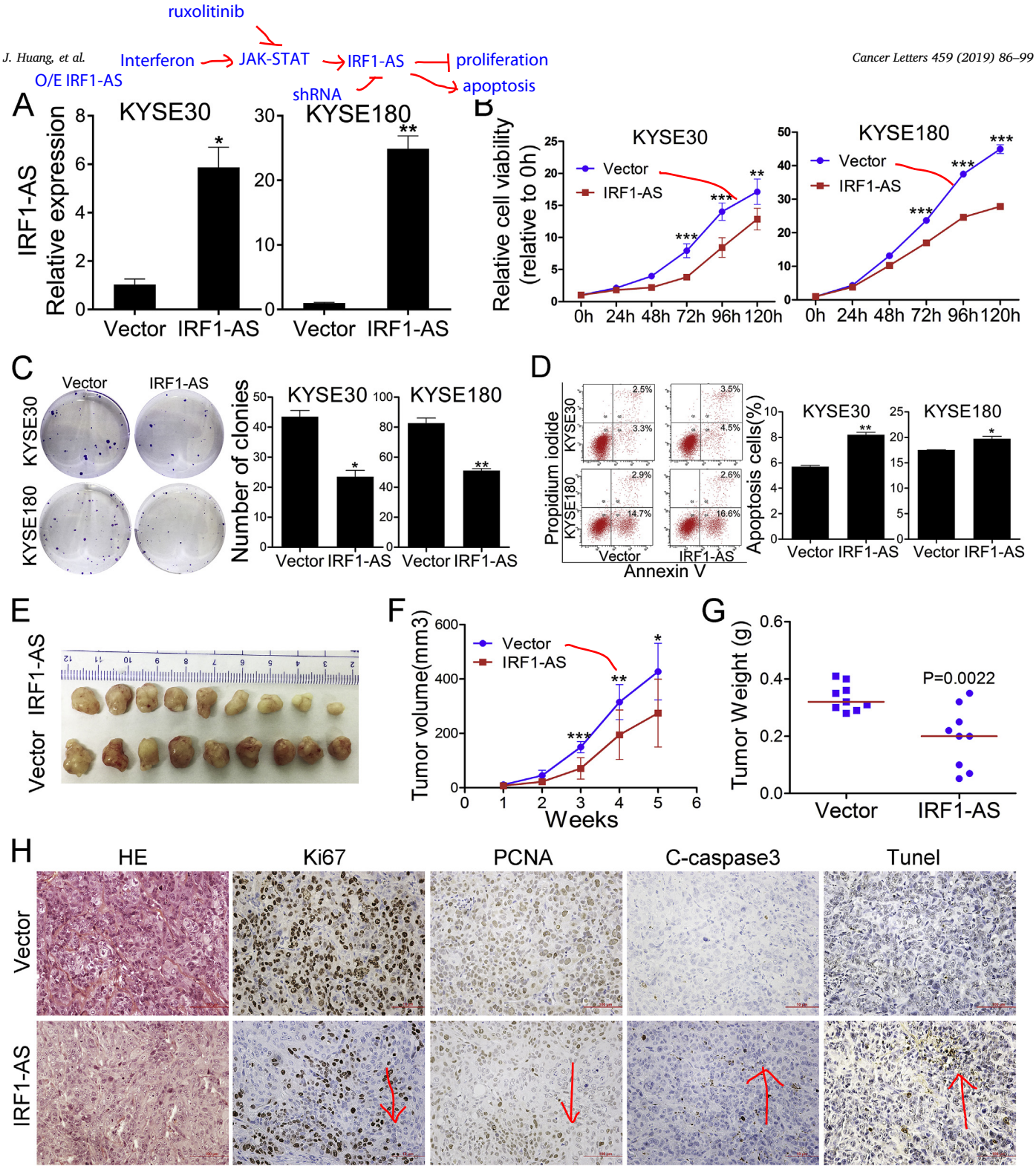

Fig. 3. Overexpression of IRF1-AS inhibits ESCC proliferation and promotes apoptosis in vitro and in vivo. (A) Validation of IRF1-AS overexpression efficiency by RT-qPCR. (B) Proliferation assays of overexpression cells and vector control cells. (C) Colony formation assays of IRF1-AS overexpression cells. The right panel shows the quantification results. (D) FACS analysis of the effect of IRF1-AS overexpression on cell apoptosis. (E) Images, (F) volumes and (G) weights of xenografts established by SC transplantation with IRF1-AS–overexpressing and control KYSE30 cells. (H) Representative images of hematoxylin and eosin (H&E), immunohistochemistry (IHC) and terminal deoxynucleotidyl transferase dUTP nick end labeling (TUNEL) staining of paraffin-embedded sections obtained from xenografts. C-caspase 3, cleaved caspase 3. Original magnification × 200. The data are shown as the mean ± SD. ***P < 0.001, **P < 0.01, *P < 0.05.

3.3. IRF1-AS activates IRF1 transcription through interacting with ILF3 and DHX9

To further investigate the interplay between IRF1-AS and IRF1, we found that both the mRNA and protein levels of IRF1 were decreased in the IRF1-AS knockdown cells (Fig. 4A) and increased in the IRF1-AS overexpression cells (Fig. 4B). A previous study reported that antisense lncRNA could form an RNA duplex with mRNA through overlapping regions to increase mRNA stability [20]. To test whether IRF1 mRNA stability was augmented by IRF1-AS, we used α-amanitin, which is an inhibitor of RNA polymerase II, to block new RNA synthesis in ESCC cells and then measured the subsequent levels of IRF1 mRNA. The

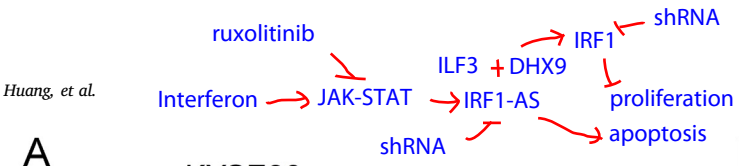

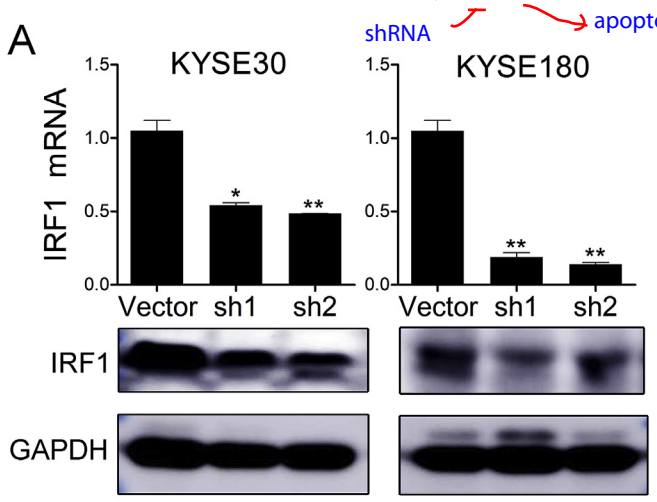

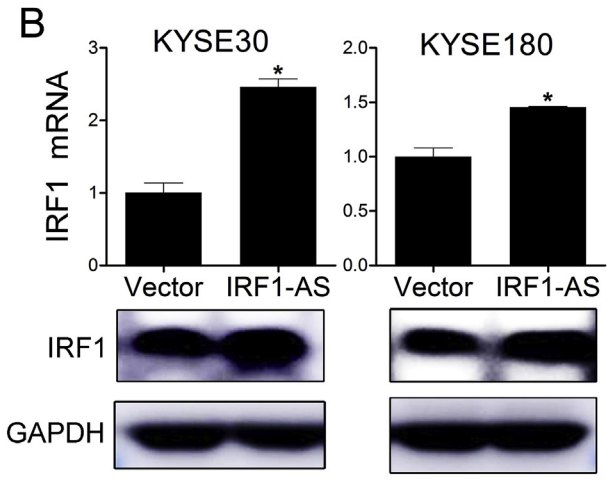

C mass spectrometry

RNA pull-down and mass spectrometry

Protein name	Sequence coverage (%)	Counts (IRF1-AS)	Counts (negative)
MCCC2	39.61	26	0
DHX9	13.39	19	0
ILF3	26.23	18	0
DSP	5.92	17	0
MCCC1	20.67	16	0

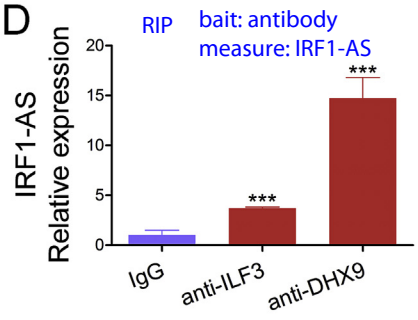

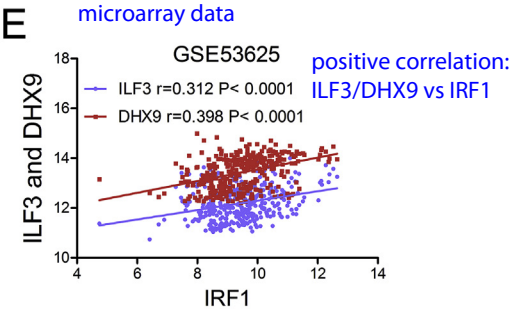

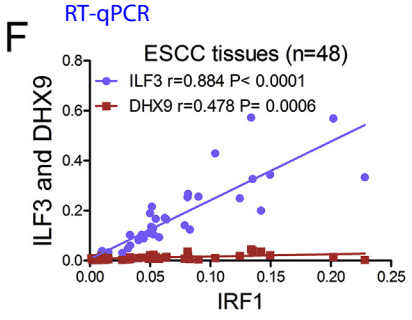

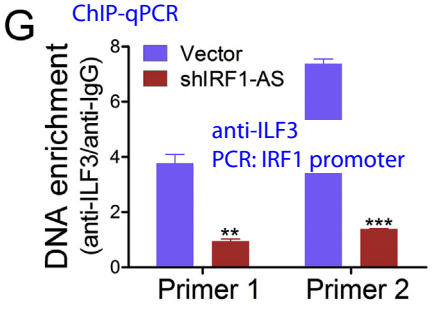

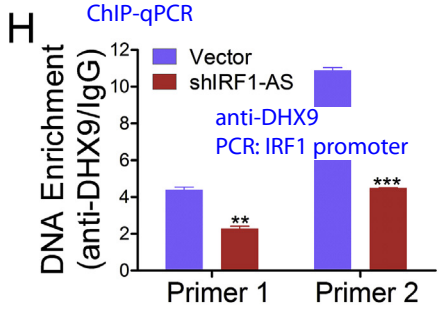

without IRF1-AS, the binding between ILF3/DHX9 and IRF1 decrease

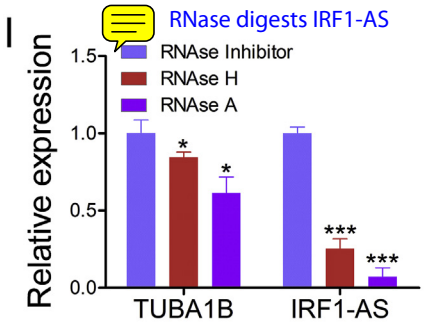

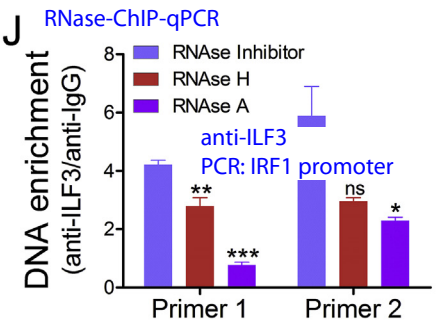

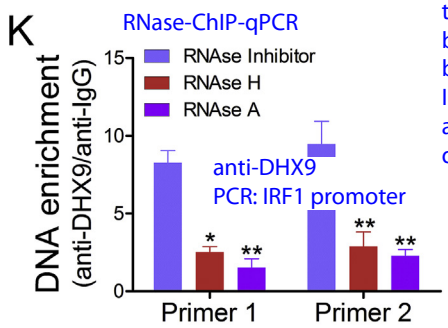

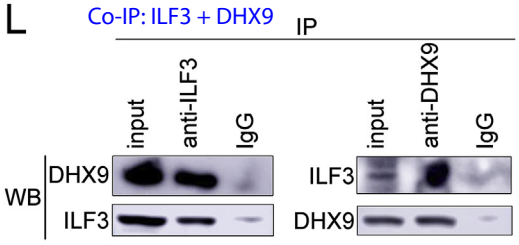

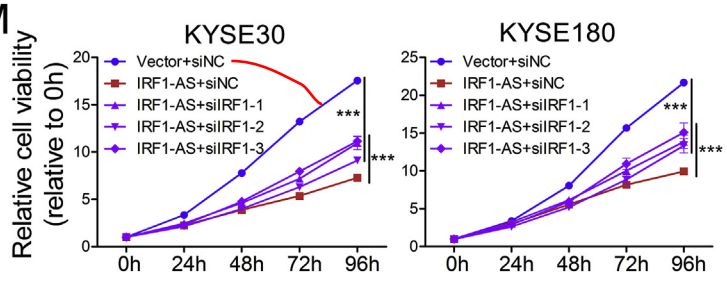

(caption on next page)

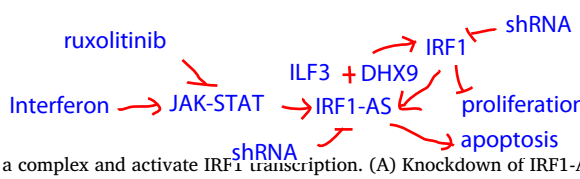

Fig. 4. IRF1-AS, ILF3 and DHX9 form a complex and activate IRF1 transcription. (A) Knockdown of IRF1-AS downregulates IRF1 expression at both the mRNA and protein levels. Upper panel, mRNA level; lower panel, protein level. (B) Overexpression of IRF1-AS upregulates IRF1 expression at both the mRNA and protein levels. (C) IRF1-AS-binding proteins with top matching scores identified by mass spectrometry. (D) Validation of IRF1-AS binding to ILF3 and DHX9 by RIP assays. (E) and (F) Correlations among IRF1, ILF3 and DHX9 mRNA levels in the microarray data (E) and RT-qPCR results (F). (G) and (H) ChIP-qPCR assays using anti-ILF3 (G) and anti-DHX9 (H) antibodies in IRF1-AS-knockdown and control KYSE30 cells. Primers specific for IRF1 promoter were used for ChIP-qPCR. (I) RNase assay for the detection of IRF1-AS and alpha-tubulin mRNA (TUBA1B) using RT-qPCR in permeabilized KYSE30 cells treated with an RNase inhibitor, RNase H or RNase A. Alpha-tubulin mRNA was used as a control. The relative expression in the two RNase treatment groups was normalized to that in the RNase inhibitor group. (J) and (K) RNase-ChIP assay with anti-ILF3 (J) and anti-DHX9 (K) antibodies in permeabilized KYSE30 cells treated with either the RNase inhibitor, RNase H or RNase A. (L) Immunoprecipitation using anti-ILF3 and anti-DHX9 antibodies with cellular lysates from KYSE30 cells. (M) Rescue effect on proliferation by siRNA-mediated IRF1 knockdown in IRF1-AS overexpression cells. The data are shown as the mean ± SD. ***P < 0.001, **P < 0.01, *P < 0.05.

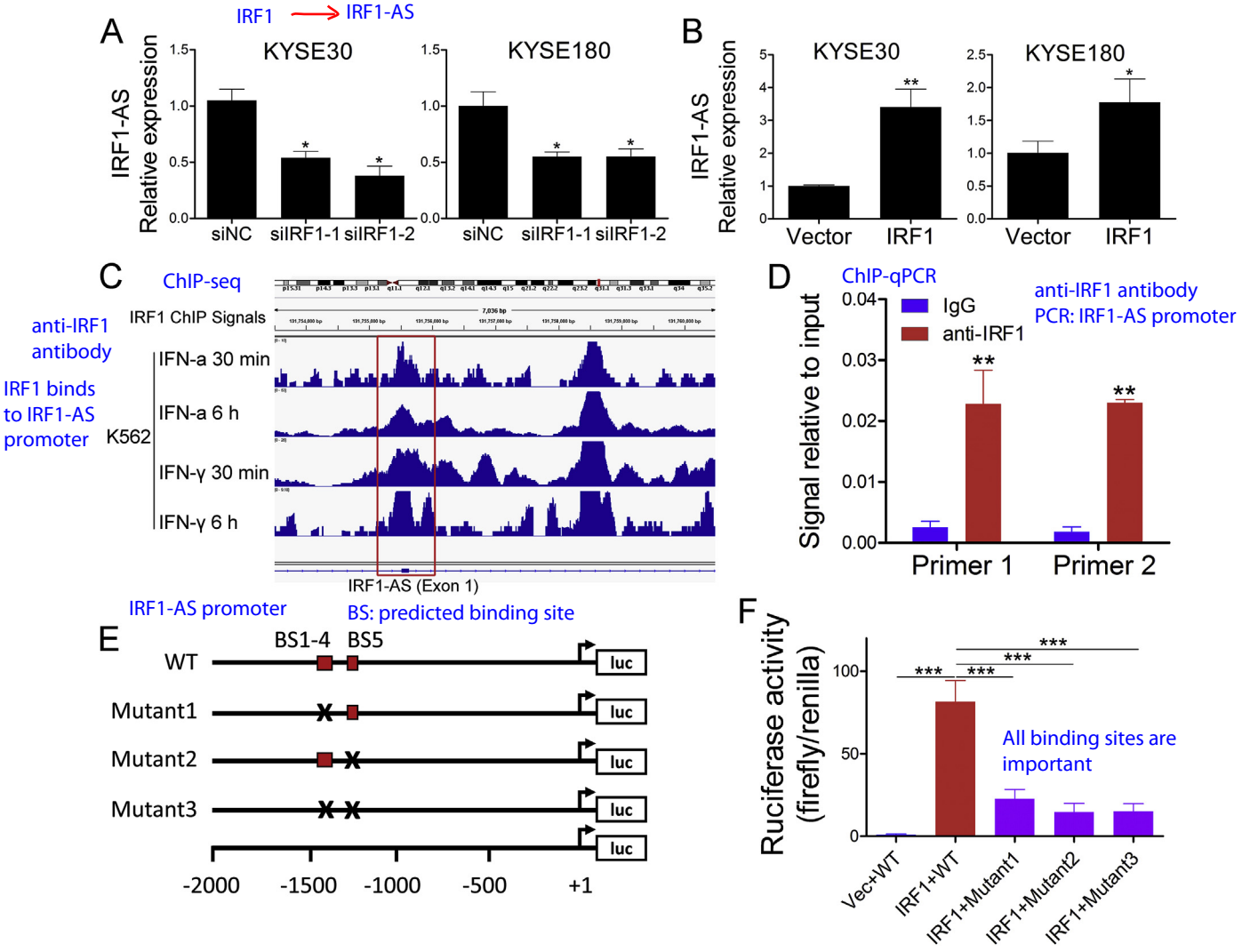

Fig. 5. IRF1 activates the transcription of IRF1-AS. (A) siRNA-mediated IRF1 knockdown downregulates IRF1-AS. (B) Overexpression of IRF1 upregulates IRF1-AS. (C) ChIP-seq results using an anti-IRF1 antibody in K562 cells following different treatments from the ENCODE project. (D) ChIP-qPCR assay using an anti-IRF1 antibody. (E) Schematic representation of the mutant construction of the IRF1-AS promoter in the dual-luciferase assay. “BS”, predicted binding site, “WT”, wild type IRF1-AS promoter. “ × ”, deletion mutation. Primers specific for ChIP-seq signal peak were used for ChIP-qPCR. (F) Relative luciferase activities of reporters containing the IRF1-AS promoter or mutants 48 h after cotransfection with the IRF1 overexpression plasmid or vector (Vec). Firefly luciferase activity was normalized to the control Renilla luciferase activity. The data are shown as the mean ± SD. ***P < 0.001, **P < 0.01, *P < 0.05.

results showed that the knockdown or overexpression of IRF1-AS had no significant effects on the IRF1 mRNA levels (Supplementary Fig. S8).

To further investigate the possible mechanism by which IRF1-AS upregulates IRF1, we performed RNA pull-down and mass spectrometry assays to detect IRF1-AS interacting proteins. According to the mass spectrometry results, we found that ILF3 (Interleukin Enhancer Binding Factor 3) and DHX9 (DExH-Box Helicase 9) were enriched exclusively in the IRF1-AS group and ranked at the top (Fig. 4C). ILF3 and DHX9 are both located in the nucleus and have RNA-binding motifs [21,22]. Moreover, ILF3 and DHX9 are associated with each other and function as transcriptional co-activators [23]. Therefore, we hypothesized that IRF1-AS interacts with ILF3 and DHX9 to transcriptionally activate IRF1. Then, we immunoprecipitated endogenous ILF3 and DHX9 to determine whether ILF3 and DHX9 interact with IRF1-AS in vivo. IRF1-AS was detected in the complexes immunoprecipitated using both anti-ILF3 and anti-DHX9 antibodies (Fig. 4D).

To unravel the potential transcriptional regulation of IRF1 by ILF3 and DHX9, we first analyzed the correlation between ILF3/DHX9 and IRF1. The results revealed that both ILF3 and DHX9 were significantly positively correlated with IRF1 in our previous microarray data [24]

Cancer Letters 459 (2019) 86–99

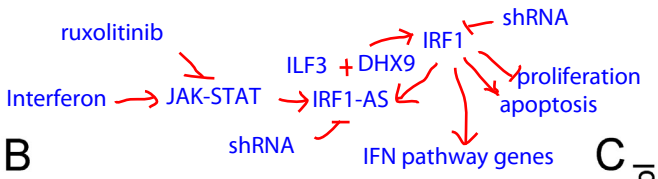

FDR <0.25; NES >=1.0; Norm P-val <0.05

A RNA-seq of IRF1-AS stable-knockdown cells

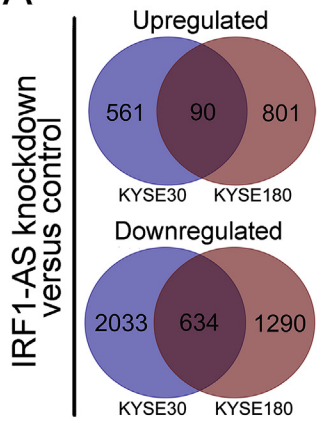

B

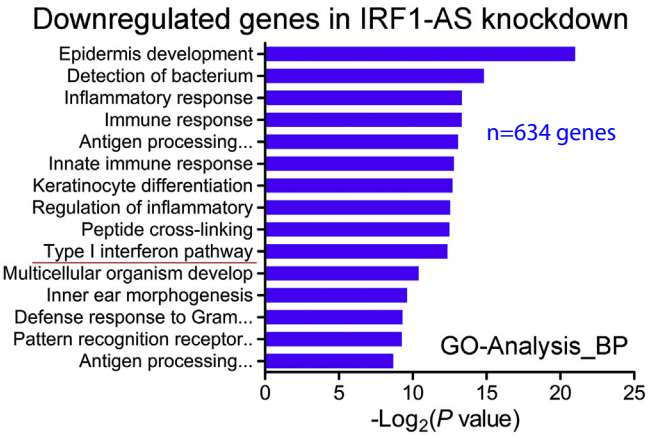

C Gene set enrichment analysis (GSEA)

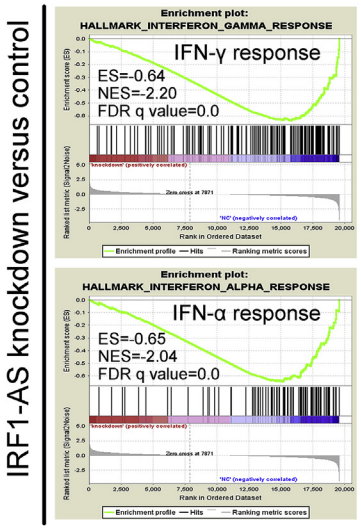

D IFN pathway genes

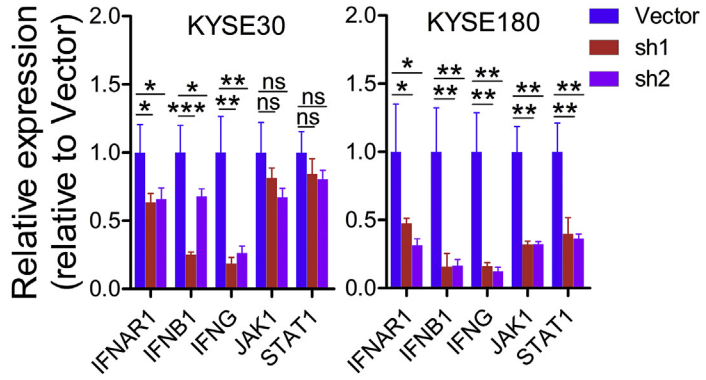

E

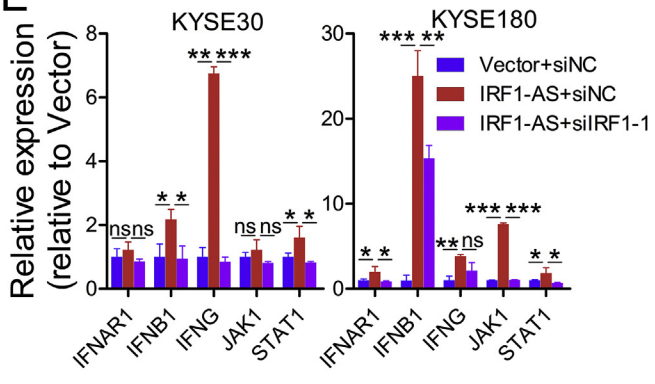

F

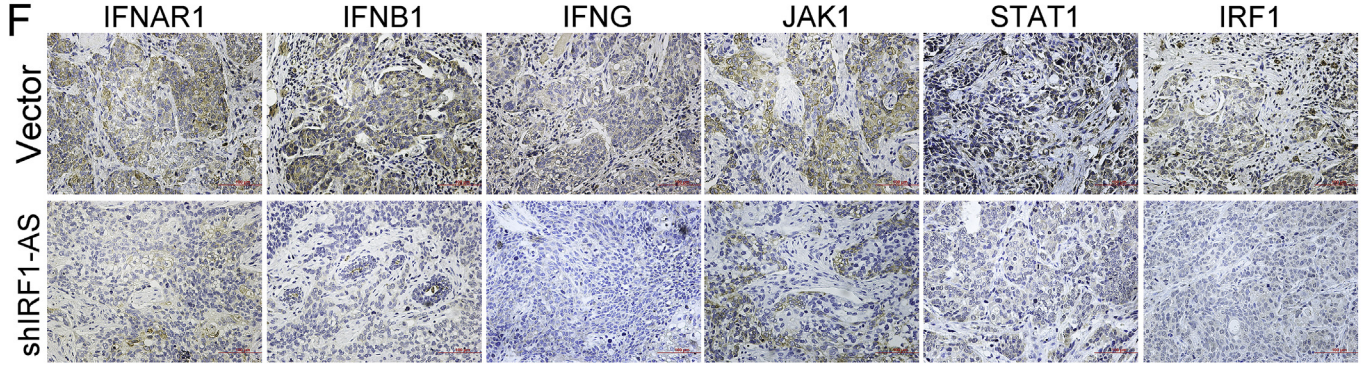

G

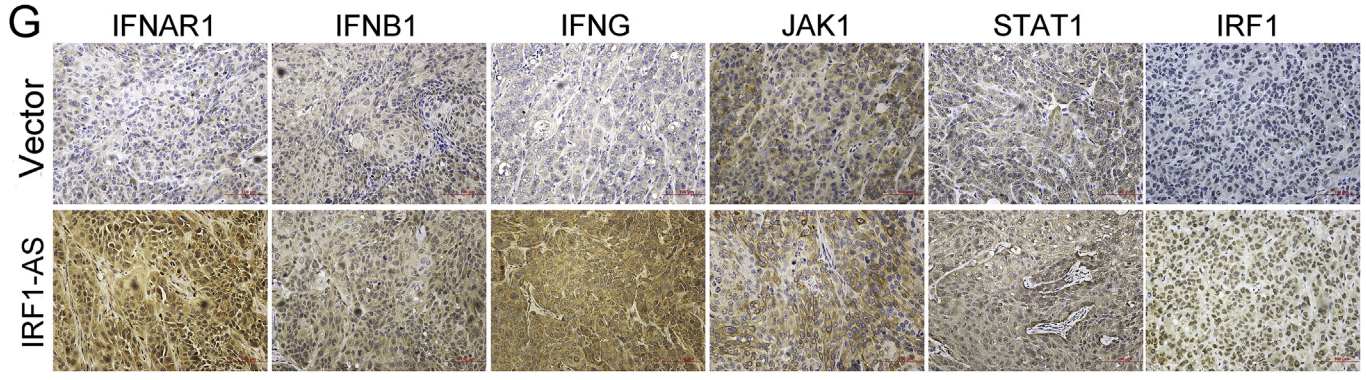

(caption on next page)

Fig. 6. Global mRNA analysis revealing that IRF1-AS regulates IFN responses. (A) RNA-seq of IRF1-AS stable-knockdown cells. Graph depicting the upregulated (FC > 2) and downregulated (FC < 2) genes after the IRF1-AS knockdown. (B) Gene Ontology analysis of the 634 downregulated genes. (C) Gene set enrichment analysis (GSEA) of IRF1-AS knockdown cells versus control cells. ES, enrichment score; NES, normalized enrichment score; FDR, false discovery rate. (D) RT-qPCR analysis of IFN pathway genes in IRF1-AS knockdown KYSE30 and KYSE180 cells. (E) Rescue effects on the expression levels of IFN pathway genes by siRNA-mediated IRF1 knockdown in IRF1-AS–overexpressing KYSE30 and KYSE180 cells. (F) Representative images of IHC staining of IFN pathway genes and IRF1 in xenografts obtained from IRF1-AS knockdown and control cells. (G) Representative images of IHC staining of IFN pathway genes and IRF1 in xenografts obtained from IRF1-AS–overexpressing and control cells. Original magnification × 200. The data are shown as the mean ± SD. ***P < 0.001, **P < 0.01, *P < 0.05. ns, not significant.

(Fig. 4E) and RT-qPCR analysis of 48 ESCC tissues (Fig. 4F). Then, we found several potential binding sites (BSs) (CTGTT) for ILF3 in the IRF1 promoter region [25]. To determine whether ILF3 and DHX9 bind the IRF1 promoter, we performed ChIP-qPCR assays. The results indicated that the IRF1 promoter sequences were significantly enriched in the anti-ILF3 (Fig. 4G) and anti-DHX9 (Fig. 4H) immunoprecipitated complexes, and the knockdown of IRF1-AS decreased the DNA enrichment (Fig. 4G and H). A previous study demonstrated that lncRNA binds chromatin and promotes the recruitment of proteins, such as lncRNA ANRASSF1 [26]. To determine whether IRF1-AS interacts with the IRF1 promoter and promotes the recruitment of ILF3 and DHX9, we treated KYSE30 cells with RNase A or RNase H, which digest single strand RNA or RNA/DNA hybrids, respectively. First, we found that both the RNase A and RNase H treatments decreased the IRF1-AS levels (Fig. 4I). Alpha-tubulin RNA, which was mainly digested by RNase A (Fig. 4I), was chosen as a control in this study. Following the RNase treatment, we performed a ChIP-qPCR assay. The results showed that both the RNase A and RNase H treatments decreased the binding of ILF3 (Fig. 4J) and DHX9 (Fig. 4K) to the IRF1 promoter. These results suggest that IRF1-AS interacts with the DNA sequence and promotes the binding of ILF3 and DHX9 to the IRF1 promoter. Subsequently, we confirmed that ILF3 and DHX9 interact with each other in vivo by performing co-immunoprecipitation assays (Fig. 4L). We also found that the knockdown and overexpression of IRF1-AS had no significant effects on the protein levels of ILF3 and DHX9 (Supplementary Fig. S9), suggesting that IRF1-AS acts only as a scaffold for ILF3 and DHX9. Collectively, IRF1-AS, ILF3 and DHX9 may form a complex and activate the transcription of IRF1.

Previous studies indicate that IRF1 can inhibit cell proliferation and induce cell apoptosis [16]. Therefore, we hypothesized that the antitumor effects of IRF1-AS depended on IRF1. We found that the siRNA-mediated knockdown of IRF1 in the IRF1-AS overexpression cells could partially abolish the antiproliferative effect of IRF1-AS (Fig. 4M). These results suggest that the antitumor effects of IRF1-AS may partly depend on IRF1.

3.4. IRF1 binds the IRF1-AS promoter and promotes IRF1-AS transcription

As a transcription factor, IRF1 can activate the transcription of IFNs and many ISGs, inducing a typical IFN response [16]. Therefore, we hypothesized that IRF1 activates the transcription of IRF1-AS. We found that the siRNA-mediated knockdown of IRF1 decreased the expression level of IRF1-AS (Fig. 5A) and that the transient overexpression of IRF1 increased the IRF1-AS levels (Fig. 5B).

Subsequently, we analyzed the promoter sequence of IRF1-AS and identified several previously reported IRF1 binding core sequences (GAAAs) in this region (Supplementary Fig. S10A) [27]. Moreover, we used the Jaspar online database to predict the BSs of IRF1 in the IRF1-AS promoter. We found five predicted BSs in the IRF1-AS promoter region, all of which contain the IRF1 binding core sequence (Supplementary Fig. S10B). Then, we retrieved the ChIP-seq results using an anti-IRF1 antibody from the ENCODE project and found that IRF1 has binding peaks around the IRF1-AS promoter region in K562 cells following different stimulations (Fig. 5C). Then, we performed a ChIP-qPCR assay and found that IRF1 could indeed bind the IRF1-AS promoter (Fig. 5D). To further confirm that IRF1 could activate the transcription of IRF1-AS and determine the possible BSs, we constructed and inserted a wild-type and mutant IRF1-AS promoter sequence into a pGL4.10 vector containing luciferase genes. The mutant construction of the IRF1-AS promoter is shown in Fig. 5E. Predicted BSs 1 to 4 had overlapping regions; thus, we constructed a deletion mutation of these four BSs simultaneously. The results of the dual luciferase reporter gene assays showed that IRF1 remarkably increased the luciferase activity, and the deletion of the predicted BSs significantly decreased the luciferase activities (Fig. 5F). Taken together, these results indicate that IRF1 directly binds the IRF1-AS promoter and activates the transcription of IRF1-AS.

3.5. IRF1-AS activates the interferon response in vitro and in vivo

To globally investigate the IRF1-AS-regulated genes and pathways, we performed an RNA-seq analysis of IRF1-AS knockdown cells and control cells. We identified 90 common upregulated genes (fold change > 2) and 634 downregulated genes (fold change > 2) in the KYSE30 and KYSE180 cell lines (Fig. 6A). Then, we determined that the downregulated genes were related to the type I interferon pathway and immune response (Fig. 6B) using DAVID online tools [28]. The GSEA also demonstrated an enrichment in the interferon response (Fig. 6C).

Therefore, we performed an RT-qPCR analysis of the IRF1-AS knockdown and overexpression cells to analyze the IFN pathway genes, including IFNAR1(interferon alpha and beta receptor subunit 1), IFNB1(interferon beta 1), IFNG (interferon gamma), JAK1 (janus kinase 1), and STAT1 (signal transducer and activator of transcription 1), which reflect the activity of the IFN response [15]. We noted that the overall expression levels of these genes were decreased in the IRF1-AS knockdown KYSE30 cells and KYSE180 cells (Fig. 6D). Moreover, the overall expression levels of these genes were increased in the IRF1-AS–overexpressing KYSE30 and KYSE180 cells (Fig. 6E), which was rescued by the IRF1 knockdown (Fig. 6E). To further confirm the regulation of the IFN response by IRF1-AS in vivo, we detected the activities of IFN pathway genes and IRF1 in xenografts obtained from IRF1-AS knockdown or overexpression cells using IHC. We found that the overall expression levels of IFN pathway genes and IRF1 were decreased in the IRF1-AS knockdown tumors (Fig. 6F) and increased in the IRF1-AS overexpression tumors (Fig. 6G). Collectively, these findings indicate that IRF1-AS activates the IFN response in vitro and in vivo, which may depend on IRF1.

3.6. IRF1-AS downregulation predicts a poor clinical outcome in ESCC patients

To further evaluate the clinical significance of IRF1-AS in ESCC, we first detected the expression level of IRF1-AS in 8 ECSS cell lines and 1 esophageal epithelium cell line, i.e., Het-1A. The results indicated that IRF1-AS was downregulated in all analyzed ESCC cell lines compared with that in the Het-1A cell line (Fig. 7A). Then, we used RT-qPCR to detect IRF1-AS expression in 48 ESCC tissues and 38 benign esophageal tissues. In comparison, the IRF1-AS expression was significantly lower in the ESCC tissues (Fig. 7B). Furthermore, we used ISH to examine IRF1-AS expression in an ESCC tissue microarray (TMA) of 225 patients. We correlated the IRF1-AS expression with the clinicopathological characteristics of the ESCC patients (Supplementary

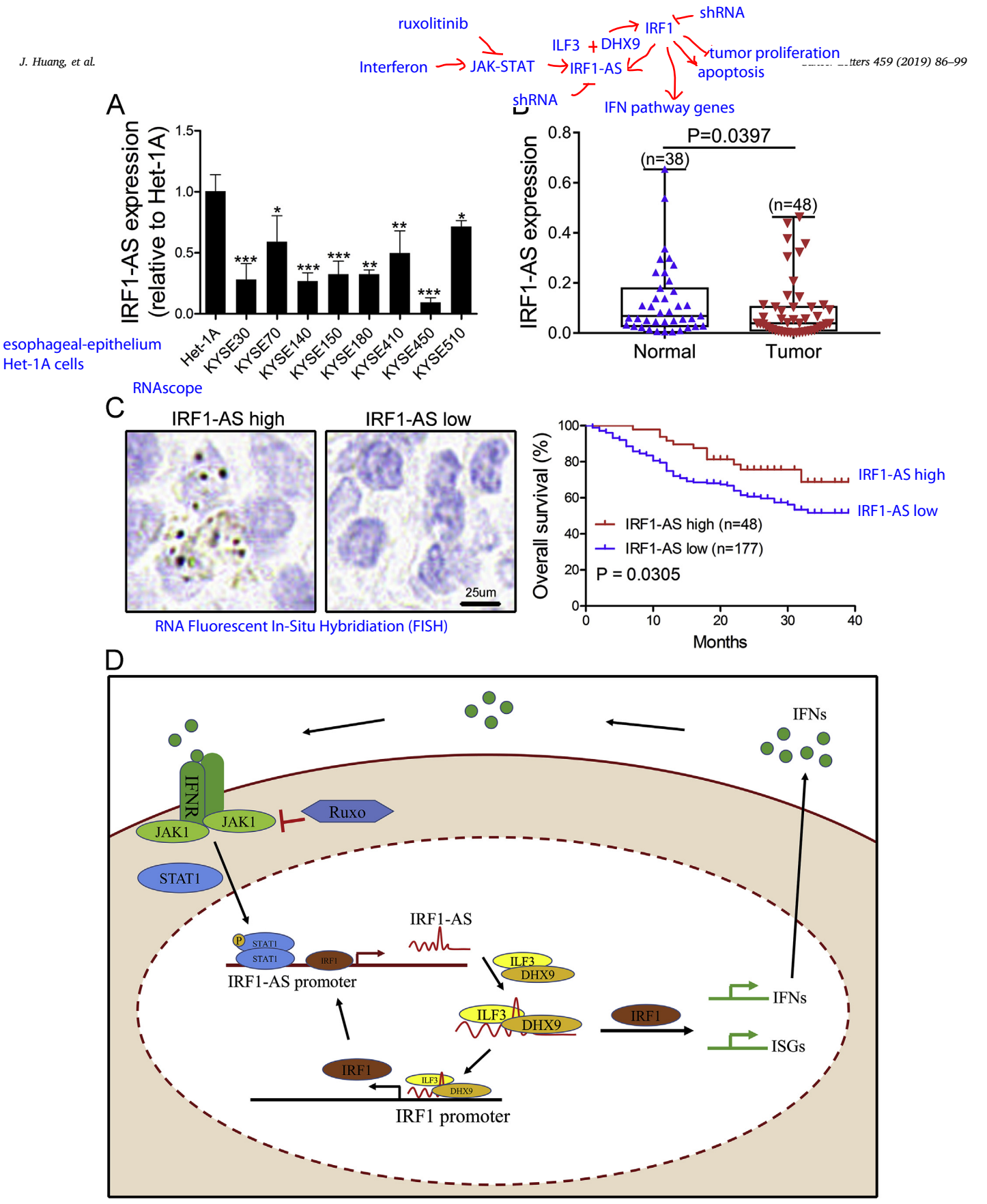

Fig. 7. Low IRF1-AS expression predicts a poor prognosis in patients with ESCC. (A) IRF1-AS expression in ESCC cell lines and esophageal-epithelium Het-1A cells as detected by RT-qPCR. (B) IRF1-AS expression in fresh-frozen ESCC tissues (n = 48) and normal esophageal tissues (n = 38) as detected by RT-qPCR. (C) Left panel, RNAscope images showing high and low IRF1-AS expression levels in ESCC tissues. Right panel, Kaplan-Meier survival curve of ESCC patients with low (score ≤ 50, n = 177) and high (score > 50, n = 48) IRF1-AS. (D) A graphical summary of the function and mechanism of IRF1-AS.

Table S3). Downregulated IRF1-AS was correlated with the TNM stage ($P < 0.05$). However, there was no significant difference in IRF1-AS expression between patients based on tumor differentiation, patient gender or age ($P > 0.05$). More importantly, the patients with low IRF1-AS expression showed a poor prognosis (Fig. 7C), and IRF1-AS was an independent prognostic factor for ESCC patients in a multivariate Cox regression analysis ($P = 0.026$, Supplementary Table S4).

4. Discussion

Interferons and their downstream pathways play pleiotropic roles in antitumor reactions. However, targeting the IFN pathway has been unsatisfactory due to unpredictable effects. Exploiting players other than known proteins involved in the IFN pathway is pivotal for targeting this pathway. In our study, we comprehensively analyzed IFN-regulated lncRNAs and identified the top-ranking candidate IRF1-AS, which functions as a positive regulator of the IFN response and a tumor suppressor in ESCC. We also identified a positive feedback loop between IRF1-AS and IRF1, which supposedly maintains the positive feedback loop between IFN signaling and IRF1-AS (Fig. 7D).

We found that interferons induce IRF1-AS expression through the JAK-STAT pathway. In addition to the classic JAK-STAT pathway, IFNs also activate the CRKL, NF-κB and MAPK pathways [19]. Therefore, whether IFNs induce IRF1-AS expression via other downstream pathways requires future investigation. The JAK-STAT pathway is a universal molecular cascade used to transduce signals for development and disease, which may be activated by a wide array of cytokines and growth factors, such as the gp130 family, βc family and γc family, in addition to IFNs [29]. Thus, a wide array of cytokines may induce IRF1-AS expression.

LncRNAs can play an oncogenic or tumor suppressive role in cancer. Here, IRF1-AS inhibited ESCC proliferation and promoted apoptosis in vitro and in vivo and acted as a tumor suppressor. Similar to many tumor suppressors, IRF1-AS was downregulated in cancer tissues and was an independent prognostic factor, highlighting its clinical implications as a biomarker. LncRNAs regulate gene expression via *cis* or *trans* mechanisms. We found that IRF1-AS upregulated IRF1 in *cis* by forming a transcription-activating complex with ILF3 and DHX9. However, the specific motifs of the IRF1-AS interaction with ILF3 and DHX9 need further investigation. Previous studies have demonstrated that IRF1 inhibits cell proliferation and induces cell apoptosis in several cancers, including esophageal cancer [16,30]. The knockdown of IRF1 rescued the antiproliferative effects of IRF1-AS, suggesting that the antitumor effects of IRF1-AS were dependent on IRF1, at least partly.

ISGs orchestrate a complex web to balance the IFN response by acting as positive or negative regulators [2]. Some studies indicate that lncRNAs regulate the IFN response through positive or negative feedback [12]. Our previous study also suggests that lncRNA GAS5 positively regulates the IFN response in ESCC [15]. Here, IRF1-AS was a positive regulator of the IFN response in vivo and in vitro. The knockdown of IRF1 in IRF1-AS overexpression cells rescued the upregulation of IFN pathway genes and IFN target genes, suggesting that IRF1 is responsible for the IRF1-AS–activated IFN response. However, whether IRF1-AS activates the IFN response via any other mechanism requires further research.

IFNs and the IFN pathway have a long history of involvement in cancer therapy. The application of IFNs in cancer treatment is mainly limited by the unpredictable IFN effects on cancer patients. There is no effective biomarker to screen patients who will benefit from IFN treatment. Considering the regulatory network among IFN signaling, IRF1-AS and IRF1, the related molecules may be potential predictive biomarkers. Furthermore, targeting the feedback loop between IRF1-AS and IRF1 to enhance the IFN response may provide a novel therapeutic strategy in cancer.

In conclusion, our results indicate that IFN-induced IRF1-AS is a tumor suppressive lncRNA that activates interferon response through a positive regulatory feedback loop with IRF1 in ESCC. Our data highlighted the interplay between the IFN-regulated lncRNA and IFN response, which forms a regulatory circuit.

Conflicts of interest

The authors declare no potential conflicts of interest.

Acknowledgements

The work was supported by the National Natural Science Foundation of China (81802299, 81502514), the Fundamental Research Funds for the Central Universities (3332018070), the CAMS Innovation Fund for Medical Sciences (CIFMS) (2016-I2M-1-001, 2017-I2M-1-005), and the National Key Basic Research Development Plan (2018YFC1312105).

Appendix A. Supplementary data

Supplementary data to this article can be found online at https://doi.org/10.1016/j.canlet.2019.05.038.

References

[1] B.S. Parker, J. Rautela, P.J. Hertzog, Antitumour actions of interferons: implications for cancer therapy, Nat. Rev. Canc. 16 (2016) 131–144.
[2] W.M. Schneider, M.D. Chevillotte, C.M. Rice, Interferon-stimulated genes: a complex web of host defenses, Annu. Rev. Immunol. 32 (2014) 513–545.
[3] V. Thorsson, D.L. Gibbs, S.D. Brown, D. Wolf, D.S. Bortone, T.H. Ou Yang, E. Porta-Pardo, G.F. Gao, C.L. Plaisier, J.A. Eddy, E. Ziv, A.C. Culhane, E.O. Paull, I.K.A. Sivakumar, A.J. Gentles, R. Malhotra, F. Farshidfar, A. Colaprico, J.S. Parker, L.E. Mose, N.S. Vo, J. Liu, Y. Liu, J. Rader, V. Dhankani, S.M. Reynolds, R. Bowlby, A. Califano, A.D. Cherniack, D. Anastassiou, D. Bedognetti, A. Rao, K. Chen, A. Krasnitz, H. Hu, T.M. Malta, H. Noushmehr, C.S. Pedamallu, S. Bullman, A.I. Ojesina, A. Lamb, W. Zhou, H. Shen, T.K. Choueiri, J.N. Weinstein, J. Guinney, J. Saltz, R.A. Holt, C.E. Rabkin, A.J. Lazar, J.S. Serody, E.G. Demicco, M.L. Disis, B.G. Vincent, L. Shmulevich, The immune landscape of cancer, Immunity 48 (2018) 812–830 e814.
[4] A. Garcia-Diaz, D.S. Shin, B.H. Moreno, J. Saco, H. Escuin-Ordinas, G.A. Rodriguez, J.M. Zaretsky, L. Sun, W. Hugo, X. Wang, G. Parisi, C.P. Saus, D.Y. Torrejon, T.G. Graeber, B. Comin-Anduix, S. Hu-Lieskovan, R. Damoiseaux, R.S. Lo, A. Ribas, Interferon receptor signaling pathways regulating PD-L1 and PD-L2 expression, Cell Rep. 19 (2017) 1189–1201.
[5] A. Ribas, J.D. Wolchok, Cancer immunotherapy using checkpoint blockade, Science 359 (2018) 1350–1355.
[6] K.V. Katlinski, J. Gui, Y.V. Katlinskaya, A. Ortiz, R. Chakraborty, S. Bhattacharya, C.J. Carbone, D.P. Beiting, M.A. Girondo, A.R. Peck, E. Pure, P. Chatterji, A.K. Rustgi, J.A. Diehl, C. Koumenis, H. Rui, S.Y. Fuchs, Inactivation of interferon receptor promotes the establishment of immune privileged tumor microenvironment, Cancer Cell 31 (2017) 194–207.
[7] K.C. Wang, H.Y. Chang, Molecular mechanisms of long noncoding RNAs, Mol. Cell 43 (2011) 904–914.
[8] M. Huarte, The emerging role of lncRNAs in cancer, Nat. Med. 21 (2015) 1253–1261.
[9] X.D. Xiong, X. Ren, M.Y. Cai, J.W. Yang, X. Liu, J.M. Yang, Long non-coding RNAs: an emerging powerhouse in the battle between life and death of tumor cells, Drug Resist. Updates : reviews and commentaries in antimicrobial and anticancer chemotherapy 26 (2016) 28–42.
[10] S. Geisler, J. Coller, RNA in unexpected places: long non-coding RNA functions in diverse cellular contexts, Nat. Rev. Mol. Cell Biol. 14 (2013) 699–712.
[11] J.L. Rinn, H.Y. Chang, Genome regulation by long noncoding RNAs, Annu. Rev. Biochem. 81 (2012) 145–166.
[12] S. Valadkhan, L.S. Gunawardane, lncRNA-mediated regulation of the interferon response, Virus Res. 212 (2016) 127–136.
[13] E. Carnero, M. Barriocanal, V. Segura, E. Guruceaga, C. Prior, K. Borner, D. Grimm, P. Fortes, Type I interferon regulates the expression of long non-coding RNAs, Front. Immunol. 5 (2014) 548.
[14] M. Barriocanal, E. Carnero, V. Segura, P. Fortes, Long non-coding RNA BST2/BISPR is induced by IFN and regulates the expression of the antiviral factor tetherin, Front. Immunol. 5 (2014) 655.
[15] J. Huang, Y. Li, Z. Lu, Y. Che, S. Sun, S. Mao, Y. Lei, R. Zang, N. Li, N. Sun, J. He, Long non-coding RNA GAS5 is induced by interferons and plays an antitumor role in esophageal squamous cell carcinoma, Cancer Med 7 (7) (2018) 3157–3167.
[16] A. Kroger, K. Koster M Fau - Schroeder, H. Schroeder K Fau - Hauser, P.P. Hauser H Fau - Mueller, P.P. Mueller, Activities of IRF-1, J. Interferon Cytokine Res. 22 (1) (2002) 5–14.
[17] J. Li, L. Han, P. Roebuck, L. Diao, L. Liu, Y. Yuan, J.N. Weinstein, H. Liang, TANRIC: an interactive open platform to explore the function of lncRNAs in cancer, Cancer

Res. 75 (2015) 3728–3737.
[18] M.F. Lin, I. Jungreis, M. Kellis, PhyloCSF: a comparative genomics method to distinguish protein coding and non-coding regions, Bioinformatics 27 (2011) i275–282.
[19] S. Hervas-Stubbs, J.L. Perez-Gracia, A. Rouzaut, M.F. Sanmamed, A. Le Bon, I. Melero, Direct effects of type I interferons on cells of the immune system, Clin. Cancer Res. 17 (2011) 2619–2627.
[20] M.A. Faghihi, F. Modarresi, A.M. Khalil, D.E. Wood, B.G. Sahagan, T.E. Morgan, C.E. Finch, G. St Laurent 3rd, P.J. Kenny, C. Wahlestedt, Expression of a noncoding RNA is elevated in Alzheimer's disease and drives rapid feed-forward regulation of beta-secretase, Nat. Med. 14 (2008) 723–730.
[21] S. Castella, R. Bernard, M. Corno, A. Fradin, J.C. Larcher, Ilf3 and NF90 functions in RNA biology, Wiley interdisciplinary reviews, RNA 6 (2015) 243–256.
[22] T. Lee, J. Pelletier, The biology of DHX9 and its potential as a therapeutic target, Oncotarget 7 (2016) 42716–42739.
[23] T.W. Reichman, A.M. Parrott, I. Fierro-Monti, D.J. Caron, P.N. Kao, C.G. Lee, H. Li, M.B. Mathews, Selective regulation of gene expression by nuclear factor 110, a member of the NF90 family of double-stranded RNA-binding proteins, J. Mol. Biol. 332 (2003) 85–98.
[24] J. Li, Z. Chen, L. Tian, C. Zhou, M.Y. He, Y. Gao, S. Wang, F. Zhou, S. Shi, X. Feng, N. Sun, Z. Liu, G. Skogerboe, J. Dong, R. Yao, Y. Zhao, J. Sun, B. Zhang, Y. Yu, X. Shi, M. Luo, K. Shao, N. Li, B. Qiu, F. Tan, R. Chen, J. He, LncRNA profile study reveals a three-lncRNA signature associated with the survival of patients with oesophageal squamous cell carcinoma, Gut 63 (2014) 1700–1710.
[25] Q. Hu, Y.Y. Lu, H. Noh, S. Hong, Z. Dong, H.F. Ding, S.B. Su, S. Huang, Interleukin enhancer-binding factor 3 promotes breast tumor progression by regulating sustained urokinase-type plasminogen activator expression, Oncogene 32 (2013) 3933–3943.
[26] F.C. Beckedorff, A.C. Ayupe, R. Crocci-Souza, M.S. Amaral, H.I. Nakaya, D.T. Soltys, C.F. Menck, E.M. Reis, S. Verjovski-Almeida, The intronic long noncoding RNA ANRASSF1 recruits PRC2 to the RASSF1A promoter, reducing the expression of RASSF1A and increasing cell proliferation, PLoS Genet. 9 (2013) e1003705.
[27] C.R. Escalante, J. Yie, D. Thanos, A.K. Aggarwal, Structure of IRF-1 with bound DNA reveals determinants of interferon regulation, Nature 391 (1998) 103–106.
[28] W. Huang da, B.T. Sherman, R.A. Lempicki, Systematic and integrative analysis of large gene lists using DAVID bioinformatics resources, Nat. Protoc. 4 (2009) 44–57.
[29] J.S. Rawlings, K.M. Rosler, D.A. Harrison, The JAK/STAT signaling pathway, J. Cell Sci. 117 (2004) 1281–1283.
[30] Y. Wang, D.P. Liu, P.P. Chen, H.P. Koeffler, X.J. Tong, D. Xie, Involvement of IFN regulatory factor (IRF)-1 and IRF-2 in the formation and progression of human esophageal cancers, Cancer Res. 67 (2007) 2535–2543.

Incorporate dUTP in 2nd strand synthesis in reverse transcription,
* Add high fidelity polymerase --> dUTP cannot be amplified
E.g., Taq DNA polymerase incorporates dUTP, but Pfu cannot tolerate dUTP
* Use uracil-DNA glycosylase (UDG) to remove dUTP-marked strand